33rd Annual International Conference of the IEEE EMBS
Boston, Massachusetts USA, August 30 - September 3, 2011

Automated Image Analysis of Cardiac Myocyte Ca^{2+} Dynamics

Robert K. Amanfu, James B. Muller, and Jeffrey J. Saucerman

Abstract— **Intracellular Ca^{2+} dynamics act as a key link between the electrical and mechanical activity of the heart. Here we present a method for high-throughput measurement, automated cell segmentation and signal analysis of Ca^{2+} transients in isolated adult ventricular myocytes. In addition to increasing experimental throughput ~10-fold compared to conventional approaches, this approach allows the study of individual cell-cell variability and relationships between Ca^{2+} signaling and cell morphology.**

I. Introduction

Ca^{2+} is a ubiquitous second messenger and is important in many cellular processes. During every heartbeat, electrical activity induces an oscillation in cytosolic Ca^{2+} called a Ca^{2+} transient, which activates the myofilaments and allows contraction. This coupling of electrical and mechanical activity is termed excitation-contraction coupling [1]. The advent of fluorescent organic dyes sensitive to changes in Ca^{2+} concentration has permitted extensive studies of how Ca^{2+} dynamics modulates excitation-contraction coupling in cardiac myocytes. These fluorescent dyes enabled substantial new insights including the role of Ca^{2+} sparks as elementary units of Ca^{2+} -induced Ca^{2+} release [2], cellular mechanisms underlying the heart's force-frequency relationships [3], and identification of spontaneous Ca^{2+} release as a trigger for cardiac arrhythmia [4].

Ca^{2+} transients can be experimentally observed by loading cells with a dye that fluoresces upon binding of released Ca^{2+} from specialized stores into the cytosol [5]. The most common method of recording the resultant fluorescent signal is to couple a photomultiplier tube (PMT) to an epifluorescence microscope [6]. The advantages of PMT's are their high sensitivity and temporal resolution. However, these advantages come at the cost of spatial resolution as fluorescence is only recorded from a single position. This limits recording to a single cell and does not allow simultaneous analysis of potentially interesting spatial features including cell size and shape or subcellular heterogeneity. Recent advances in the temporal resolution and sensitivity of charge-coupled device (CCD) cameras and raster-scanning confocal microscopes provide the opportunity to simultaneously image Ca^{2+} transients from multiple cardiac myocytes, which would greatly increase experimental throughput and enable assessment of cell-cell variability. Confocal imaging is already used to examine subcellular Ca^{2+} dynamics such as Ca^{2+} sparks and Ca^{2+} waves [7]. Imaging approaches are also used to image electrical and Ca^{2+} activity in monolayers of cultured neonatal myocytes [8]. In this study, we optimized a system for CCD-based imaging of Ca^{2+} transients in multiple adult ventricular myocytes, which increases experimental throughput ~10-fold. Accurate extraction and analysis of Ca^{2+} signals from such large data sets becomes a new bottleneck. To address this, an automated cell segmentation and shape analysis pipeline was developed. This provides rapid and objective quantification of Ca^{2+} dynamics in cell populations and the comparison of Ca^{2+} dynamics with cell shape characteristics. An overview of this approach is provided in Fig 1.

Manuscript received April 15, 2011. This work was supported in part by the American Heart Association Grant 0830470N and National Institutes of Health Grant R01HL094476 (to JJS).

Robert K. Amanfu is with the Department of Biomedical Engineering, University of Virginia, Box 800759, Charlottesville, VA 22908 (e-mail: rka2p@virginia.edu).

James B. Muller is with the Department of Biomedical Engineering, University of Virginia, Box 800759, Charlottesville, VA 22908 (e-mail: jbm9z@virginia.edu).

Jeffrey J. Saucerman is with the Department of Biomedical Engineering, University of Virginia, Box 800759, Charlottesville, VA 22908 (phone: 434-924-5095; e-mail: jsaucerman@virginia.edu). *Corresponding author

II. Materials and Methods

A. Data Acquisition

Single adult rat ventricular myocytes were isolated similar to [9] from 6 adult male (250 g) Sprague-Dawley rats. All procedures were performed in accordance with the *Guide for the Care and Use of Laboratory Animals* published by the US National Institutes of Health and approved by the University of Virginia Institutional Animal Care and Use Committee. Collagenase used for tissue digestion was obtained from Cellutron Life Technologies (Baltimore, MD).

Isolated ventricular myocytes were plated on 35 mm glass coverslips treated with 40 µg/ml laminin at a density of ~ $3x10^6$ cells per ml. Unattached cells were removed after 1 hour by aspirating and replenishing media. Cells were loaded with 1 µM fluo-4 acetoxymethyl [5] (Invitrogen, Carlsbad, CA) for 30 minutes at room temperature in a solution of MEM containing (in mM) $NaHCO_3$ 4.7, pyruvic acid 2, Na-HEPES 10, HEPES 10 and (in units/ml) insulin 0.4, and penicillin-streptomycin 50 (pH 7.35). The non-ratiometric Ca^{2+} dye fluo-4 was selected over commonly used ratiometric dyes (indo-1 and fura-2) due to its high signal-to-noise ratio and simplified imaging requirements [7]. Cells were incubated in MEM for another 30 minutes to allow for dye de-esterification. Next, they were placed in a slotted bath chamber with platinum electrical field electrodes (Warner Instruments, Hamden, CT).

Cells were imaged on an IX-81 microscope (Olympus, Center Valley, PA) with 10X (either 0.3 or 0.4 numerical aperture) objectives for CCD imaging and 40X 0.6

numerical aperture objective for PMT recording. All experiments were performed at room temperature (21-24 °C).

Ca^{2+} transients were detected with either a PMT400 system (Ionoptix, Milton, MA) or a Hamamatsu C9300 CCD camera (Bridgewater, NJ) at 8X8 binning and 15 ms exposure time. Sampling frequency was 1000 Hz and 67 Hz for the PMT and CCD camera respectively. The camera was set in stream acquisition mode using Metamorph imaging software (Molecular Devices, Sunnyvale, CA). This setting enables image acquisition at an interval approximately equal to the exposure time. Excitation light was generated using a Lambda DG4 300 watt xenon lamp (Sutter, Novato, CA), filtered through a 5% neutral density filter and 480/40 nm bandpass excitation filter. Fluorescence emission was detected using a 505 nm dichroic and 535/50 nm bandpass emission filter (Chroma, Bellows Falls, VT). The cell chamber was constantly perfused with Tyrodes solution containing (in mM) NaCl 140, KCl 4, $MgCl_2$ 1, and HEPES 10 (pH 7.4). Cells were paced with an electrical stimulator (Ionoptix, Milton, MA) at a frequency of 0.5-1 Hz with a bipolar pulse of duration 4 ms at a voltage of 10 V.

B. Automated Cell Segmentation

As shown in Fig. 2a, individual frames of an image stack contained considerable noise, particularly at diastole when $[Ca^{2+}]$ is low. The low signal-to-noise ratio makes cell segmentation difficult. To overcome this, we automatically identified and averaged image frames of maximum Ca^{2+} intensity (coinciding with the stimulation frequency of the electrical pacer) to increase the signal-to-noise ratio used for cell segmentation (see Fig. 2b). Images were then segmented using Otsu's method for threshold selection [10], which works by identifying the optimum threshold in an image's intensity histogram that minimizes the variance between pixels in the background and foreground (Fig. 2c). Using this threshold, a mask image was created with identified regions of interest (ROIs). An example of the resulting segmented ventricular myocytes is shown in Fig. 2d.

C. Ca^{2+} Signal Analysis

The resulting regions of interests (ROI's) were used to extract each cell's fluorescence intensity at each time point (or acquired image). Background signal at each timepoint was quantified by taking the average intensity of all regions below the segmentation threshold. Raw fluorescence values were background-subtracted and then normalized to diastolic Ca^{2+} intensity Fo as (F-Fo)/Fo, or $\Delta F/Fo$. Averaged Ca^{2+} transients were calculated by averaging 5 consecutive transients. Diastolic and systolic values are estimated by finding the minimum and maximum intensities of the averaged transient. An estimate of the relaxation time (signal decay) was obtained by identifying the time at which normalized fluorescence intensity is 50% of the max amplitude. All segmentation and feature extraction was implemented in MATLAB (The Mathworks, Natick MA). MATLAB code for these analyses and example movies are freely available at http://bme.virginia.edu/saucerman.

III. RESULTS

A. CCD-based imaging of Ca^{2+} transients

To determine the image acquisition rate necessary to adequately sample Ca^{2+} transient signals, Ca^{2+} transients were measured at 1000 Hz using the PMT system and then downsampled to simulate various CCD camera sampling frequencies (Fig. 3a). During CCD-based image acquisition each pixel well integrates the photons hitting the detector during the exposure time, essentially averaging the signal. To simulate these effects of photon integration during CCD acquisition at various sampling frequencies, a moving average filter with width corresponding to the exposure time was used (for example a 10 Hz sampling rate corresponds to 100 ms exposure time on a CCD camera). Spectral analysis of the 1000 Hz PMT signal indicates that the Ca^{2+} signal bandwidth is ~ 14.4 Hz (Fig. 3b), corresponding to a Nyquist sampling rate of 28.8 Hz. Thus an image acquisition frequency of 67 Hz is sufficient to minimize aliasing artifact.

Qualitatively, aliasing is evident at lower sampling frequencies as shown in Fig. 3a, especially at 10 Hz. Quantification of Ca^{2+} transient parameters amplitude and decay rate (t_{50}) is shown in Fig. 3c-d. While these graphs alone suggests that even 67 Hz down-sampling rates underestimates those parameters, inspection of the inset in Fig. 3a demonstrates that the larger Ca^{2+} transient amplitude seen with 1000 Hz sampling is largely an artifact of larger signal noise in the PMT. Thus photon integration occurring on the CCD camera acts as a low-pass filter.

We then used the CCD camera system to record Ca^{2+} transients from adult ventricular myocytes at 67 Hz sampling and image exposure time of 15 ms. As described in Methods and Materials, automated cell segmentation was performed to identify individual myocytes and Ca^{2+} signals were normalized to obtain signals as shown in Fig. 4. This demonstrates that Ca^{2+} transients can be simultaneously measured from multiple cardiac myocytes with reasonably high signal-to-noise. We found that using this approach, ~7% photobleaching occurs in 60 sec of continuous imaging. Restricting imaging to 10 sec intervals every 1 minute enabled longer-term observation of Ca^{2+} signals.

B. Ventricular Myocyte Shape Analysis

Using the Image Processing Toolbox in MATLAB, morphologic parameters were quantified automatically from 333 myocytes including cell area, major and minor axis lengths (fitted to an ellipse). As shown in Fig. 5a, myocytes had a median cell area of 1.55×10^3 μm^2, but the distribution of cells exhibits substantial variability and a long tail with several much larger myocytes. Note that overlapping myocytes erroneously segmented as a single cell (as in the upper-center of Fig. 2d) were manually excluded from this analysis, but could be identified automatically in the future. The ratio of major to minor axis lengths is a simple measure of cell shape. The distribution of major-minor axis length ratios shows two distinct populations of cells corresponding to rod-shaped and hypercontracted cells (for example cell 2 in Fig. 4), with the former more commonly described as being healthy, normal myocytes [11]. Isolated ventricular

myocytes can become hypercontracted when overloaded by Ca^{2+}, typically no longer exhibiting normal Ca^{2+} dynamics.

Combining the information provided by Ca^{2+} signals and cell morphology may provide new insights into myocyte function. Comparison of Ca^{2+} dynamics and major-minor axis ratio may enable identification of unhealthy cells that should be excluded from subsequent analysis. Further, there may be relationships between cell size, shape and Ca^{2+} signaling within the rod-shaped myocyte population. For example, myocytes isolated from failing hearts are hypertrophied (enlarged), and swelling of cardiac myocytes is a known aspect of ischemia-reperfusion [12]. Both of these conditions are typically associated with decreased Ca^{2+} transient magnitude.

Here, we examined relationships between Ca^{2+} transient amplitude, myocyte area, and major-minor axis ratio in normal ventricular myocytes. As shown in Fig. 6a, Ca^{2+} transient amplitudes varied considerably from cell to cell, even when in the same experiment and field of view. However, Ca^{2+} transient amplitude was not correlated with cell area (Pearson correlation coefficient r = .14), indicating that cell size is not a substantial determinant of Ca^{2+} transients within this myocyte population. Given previous data on the effects of acute cell swelling on Ca^{2+} transients [12], this could indicate that myocytes regulate ion channel expression to maintain normal Ca^{2+} transients.

Fig. 6b shows the relationship between major-minor axis ratio and Ca^{2+} transient amplitude in myocytes. Rounded or hypercontracted myocytes typically had very small or no Ca^{2+} transients and were typically arrhythmic (i.e. displaying abnormal calcium transients). This could be a direct consequence of shortened sarcomere length as suggested by recent data investigating the causes of arrhythmia in cardiac hypertrophy [13]. Another study using engineered cardiac tissue showed that decreasing major-minor axis ratio resulted in smaller calcium amplitude [14]. More rod-shaped myocytes exhibited larger Ca^{2+} transients as expected of healthy myocytes. The normal rod-shaped population can be selected by excluding cells with a major minor axis < 2.5 and amplitude < 1 (89% of selected population display normal Ca^{2+} transients). However, even when excluding hypercontracted and the majority of arrhythmic cells, rod-shaped normal myocytes exhibited considerable variation in Ca^{2+} transients not accounted for by major-minor axis ratio alone(r =- .076).

IV. DISCUSSION

Here we developed a method for simultaneous imaging of Ca^{2+} transients in multiple adult ventricular myocytes with sufficient temporal and spatial resolution for quantitative analysis. Automated cell segmentation and Ca^{2+} signal analysis substantially increases the throughput, sensitivity, and objectivity of the approach. The improved spatial resolution also provides an opportunity to examine relationships between Ca^{2+} signaling and cell morphology.

While we did not observe appreciable correlation between cell morphology and Ca^{2+} transients in normal rod-shaped myocytes, cell shape was able to identify rounded myocytes with dysfunctional Ca^{2+} regulation. This demonstrates proof-of-principle that this approach may be subsequently extended to pathological conditions such as heart failure or ischemia where coordinated changes in cell size, shape, and Ca^{2+} signaling have been noted. More advanced measures of cell shape including eccentricity could be analyzed as well. Extensions of this approach may allow automated analysis of arrhythmic Ca^{2+} waves where Ca^{2+} signals are not uniform within the cell.

ACKNOWLEDGMENT

The authors thank Lindsay McClellan for technical assistance with myocyte isolations.

REFERENCES

[1] D. M. Bers, "Cardiac excitation-contraction coupling," *Nature*, vol. 415, no. 6868, pp. 198-205, Jan. 2002.

[2] H. Cheng, W. Lederer, and M. Cannell, "Calcium sparks: elementary events underlying excitation-contraction coupling in heart muscle," *Science*, vol. 262, no. 5134, pp. 740 -744, Oct. 1993.

[3] J. DeSantiago, L. S. Maier, and D. M. Bers, "Frequency-dependent Acceleration of Relaxation in the Heart Depends on CaMKII, but not Phospholamban," *Journal of Molecular and Cellular Cardiology*, vol. 34, no. 8, pp. 975-984, Aug. 2002.

[4] H. Cheng, M. R. Lederer, W. J. Lederer, and M. B. Cannell, "Calcium sparks and [Ca2+]i waves in cardiac myocytes," *American Journal of Physiology - Cell Physiology*, vol. 270, no. 1, p. C148 - C159, Jan. 1996.

[5] K. R. Gee, K. A. Brown, W.-N. U. Chen, J. Bishop-Stewart, D. Gray, and I. Johnson, "Chemical and physiological characterization of fluo-4 Ca2+-indicator dyes," *Cell Calcium*, vol. 27, no. 2, pp. 97-106, Feb. 2000.

[6] M. W. Nickola, L. E. Wold, P. B. Colligan, G.-J. Wang, W. K. Samson, and J. Ren, "Leptin Attenuates Cardiac Contraction in Rat Ventricular Myocytes : Role of NO," *Hypertension*, vol. 36, no. 4, pp. 501-505, Oct. 2000.

[7] S. Guatimosim, C. Guatimosim, and L.-S. Song, "Imaging calcium sparks in cardiac myocytes," *Methods in Molecular Biology (Clifton, N.J.)*, vol. 689, pp. 205-214, 2011.

[8] B. J. Darrow, V. G. Fast, A. G. Kleber, E. C. Beyer, and J. E. Saffitz, "Functional and Structural Assessment of Intercellular Communication: Increased Conduction Velocity and Enhanced Connexin Expression in Dibutyryl cAMP- Treated Cultured Cardiac Myocytes," *Circ Res*, vol. 79, no. 2, pp. 174-183, Aug. 1996.

[9] D. M. Bers, W. J. Lederer, and J. R. Berlin, "Intracellular Ca transients in rat cardiac myocytes: role of Na-Ca exchange in excitation-contraction coupling," *American Journal of Physiology - Cell Physiology*, vol. 258, no. 5, p. C944 -C954, May. 1990.

[10] "A Threshold Selection Method from Gray-Level Histograms," *Systems, Man and Cybernetics, IEEE Transactions on*, vol. 9, no. 1, pp. 62-66, 1979.

[11] S. P. Bishop and J. L. Drummond, "Surface morphology and cell size measurement of isolated rat cardiac myocytes," *Journal of Molecular and Cellular Cardiology*, vol. 11, no. 5, pp. 423-430, May. 1979.

[12] G.-R. Li and C. M. Baumgarten, "Modulation of cardiac Na+ current by gadolinium, a blocker of stretch-induced arrhythmias," *American Journal of Physiology - Heart and Circulatory Physiology*, vol. 280, no. 1, p. H272 -H279, Jan. 2001.

[13] L. T. Izu, T. Banyasz, and Y. Chen-Izu, "Sarcomere Shortening Destabilizes the Ca2+ Control System in Ventricular Myocytes: Implications for Understanding Arrhythmias in Familial Hypertrophic Cardiomyopathy," *Biophysical Journal*, vol. 96, no. 3, Supplement 1, p. 513a, Feb. 2009.

[14] T. Pong et al., "Hierarchical architecture influences calcium dynamics in engineered cardiac muscle," *Exp. Biol. Med.*, vol. 236, no. 3, pp. 366-373, Mar. 2011.

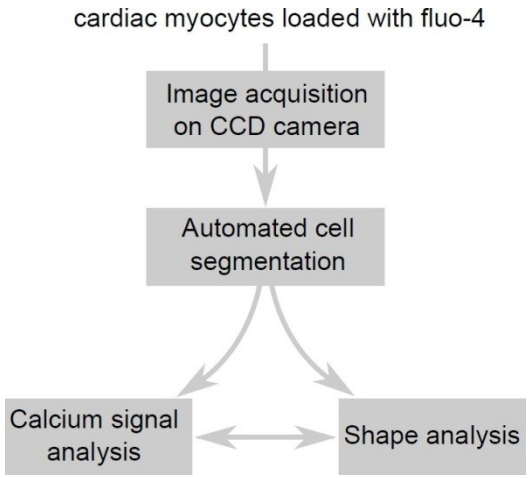

Fig. 1: Flow diagram for the proposed method

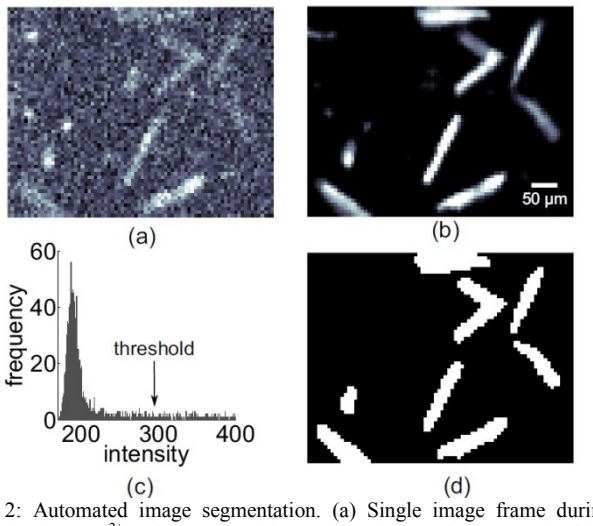

Fig. 2: Automated image segmentation. (a) Single image frame during diastole (low [Ca^{2+}]). (b) Averaged image from frames during systole (high [Ca^{2+}]. (c) Histogram of intensity values of the averaged image. The threshold is identified using Otsu's method. (d) Segmented image

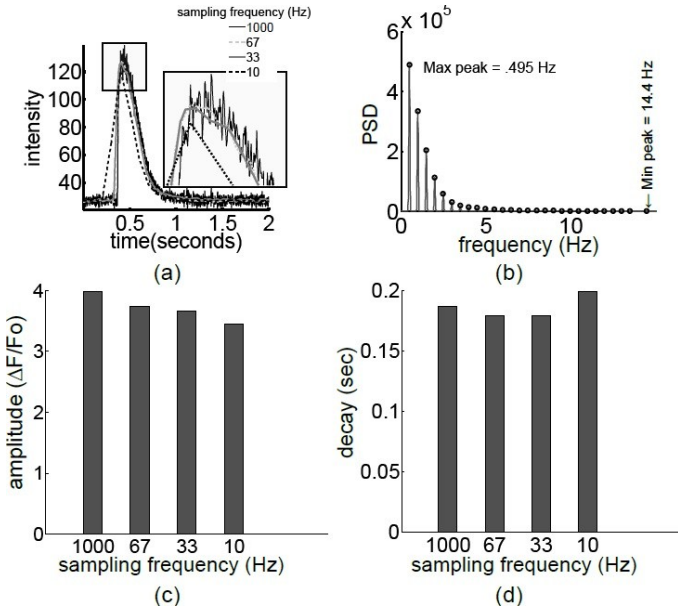

Fig. 3: Analysis of the effects of down-sampling PMT data. (a) Averaged transients of down-sampled PMT data. (b) Power spectral density (PSD) of original PMT data. The peak corresponds with the pacing frequency, and the signal has a bandwidth of ~14.4 Hz. (c) Effect of sampling frequency on amplitude of averaged Ca^{2+} transients. (d) Effect of sampling on decay time (t_{50}) of averaged Ca^{2+} transients.

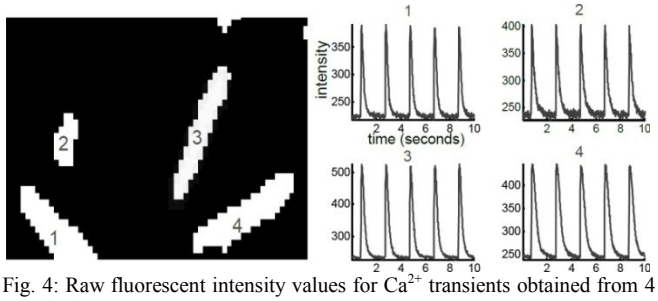

Fig. 4: Raw fluorescent intensity values for Ca^{2+} transients obtained from 4 ventricular myocyte ROI's.

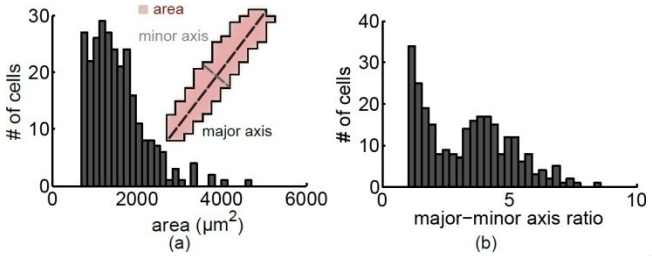

Fig. 5: Histogram of cell size and shape features calculated from automated segmentation of 333 myocytes. (a) Histogram of cell area. (b) Histogram of major-minor axis length ratio.

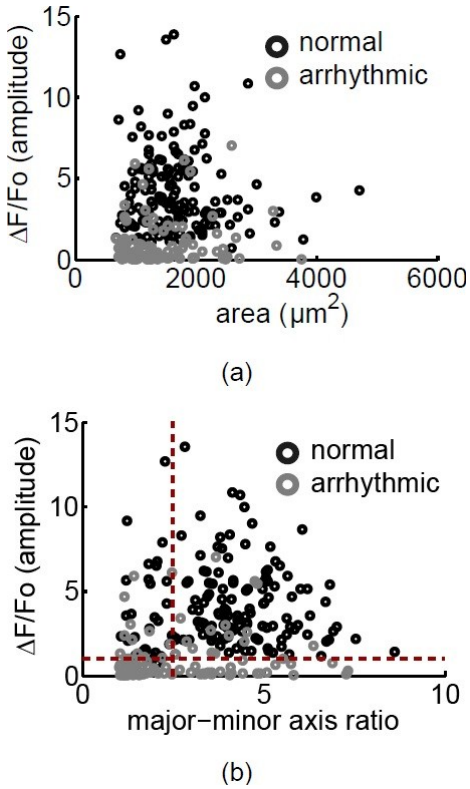

Fig. 6: Correlation plots of (a) amplitude and area ;(b) amplitude and major-minor axis ratio. Dashed lines indicate separation of cells by having Ca^{2+} transient amplitudes > 1 and major-minor axis ratio > 2.5.